Optics & Laser Technology 58 (2014) 94–99

Contents lists available at ScienceDirect

Optics & Laser Technology

journal homepage: www.elsevier.com/locate/optlastec

Investigations of morphological features of picosecond dual-wavelength laser ablation of stainless steel

Wanqin Zhao, Wenjun Wang*, Xuesong Mei, Gedong Jiang, Bin Liu

State Key Laboratory for Manufacturing Systems Engineering, Xi'an Jiaotong University, Xi'an 710049, China

A R T I C L E I N F O

Article history:
Received 5 June 2013
Received in revised form
24 September 2013
Accepted 4 November 2013
Available online 26 November 2013

Keywords:
Morphology
Picosecond laser
Dual-wavelength beam

A B S T R A C T

Investigations on the morphological features of holes and grooves ablated on the surface of stainless steel using the picosecond dual-wavelength laser system with different powers combinations are presented based on the scarce researches on morphology of dual-wavelength laser ablation. The experimental results show the profiles of holes ablated by the visible beam appear V-shaped while those for the near-infrared have large openings and display U-shaped, which are independent of the ablation mechanism of ultrafast laser. For the dual-wavelength beam (a combination of visible beam and near-infrared), the holes resemble sunflower-like structures and have smoother ring patterns on the bottom. In general, the holes ablated by the dual-wavelength beam appear to have much flatter bottoms, linearly sloped side-walls and spinodal structures between the bottoms of the holes and the side-walls. Furthermore, through judiciously combining the powers of the dual-wavelength beam, high-quality grooves could be obtained with a flat worm-like structure at the bottom surface and less resolidified melt ejection edges. This study provides insight into optimizing ultrafast laser micromachining in order to obtain desired morphology.

1. Introduction

In the last few decades, many studies have been conducted on characteristics of ultrafast lasers micromachining. Some studies have focused on laser parameters, such as fluence, wavelength, pulse duration, repetition rate and pulse number [1–4], while others have been concerned with external laser processing methods, such as changing the processing environment (from or to an ambient liquid, gas or vacuum) [5–9]. All these studies have been aimed at improving the efficiency and morphology of laser micromachining. In recent years, many researchers have adopted combined strategies, such as using dual-laser systems, dual-wavelength systems or generating pulse trains, etc., and obtained better ablation efficiency. For double-laser systems, integrated femtosecond (fs) and nanosecond (ns) dual-beam laser systems have been found to be more efficient at removing multiple materials than mono-laser systems [10–12]; in addition, another study reviewed the vacuum ultraviolet (VUV)–ultraviolet (UV) dual-laser excitation process and found that it could perform high-efficiency ablation of different materials attributing to the absorption of the UV laser by excited-states formed by the VUV laser irradiation [13]. For double-wavelength systems, one study showed that ablation efficiency could be enhanced by using prepulses (fs) of 260 nm with linear absorption followed by main pulses (fs) of 780 nm with three-photon absorption during the selected removal of insulating layers from substrate materials [14]; furthermore, micromachining with dual-wavelength system has been found to improve the aspect ratios of holes and ablation yields [15,16]. With respect to the pulse train technique, one study showed that material removal rates could be increased significantly by using a train of carefully timed pairs of nanosecond laser pulses [17].

However, for the ablated morphology also highly relevant to numerous practical applications, only a few researches have been reported as a small portion of the total papers. For example, one study did report that two lasers could be combined to create holes with sharp edges, flat side-walls and smooth bottoms [13], a few other studies showed that double-wavelength laser could ablate holes with more regular profiles and surface morphologies that appeared to be smoother [15,16]. Based on this information, dual-ablation strategies may be able to improve the morphological features of ablated structures, further, it is very necessary for the comprehensive studies on the dual-combination ablation morphology attributing to the scarcity of systematical and regular researches.

To contribute to this knowledge gap, the morphological features of dual-wavelength beam (a combination of visible beam, 532 nm and near-infrared, 1064 nm) ablation holes and grooves on

---

* Corresponding author. Tel./fax: +86 29 82663870.
E-mail address: wenjunwang@mail.xjtu.edu.cn (W. Wang).

0030-3992/$ - see front matter © 2013 Elsevier Ltd. All rights reserved.
http://dx.doi.org/10.1016/j.optlastec.2013.11.004

the surface of stainless steel are presented. In this study, a series of experiments of mono- and dual-wavelength beams ablation were performed. First, the morphological features of holes ablated by two mono-wavelengths, namely visible beam and near-infrared, were compared. Then, the morphology of hole for the dual-wavelength beam was analyzed. Subsequently, the ablation of grooves was carried out for the dual-wavelength, and the high-quality grooves were obtained by collocating double wavelengths beams powers judiciously.

2. Experiment

The stainless steel (SS304) samples as one of the most important industrial materials were used in this study. The samples were of rectangular shape with dimensions of 30 mm × 20 mm × 1.5 mm (length × width × thickness). The composition of samples was monitored by EDX (energy dispersive X-ray detector) and the elemental analysis of the SS304 surface is given in Table 1. The laser utilized for irradiation was a neodymium–vanadate (Nd:VAN; Austria laser delivering pulses with 10 ps duration, a power of 2 W and a repetition rate of 1 kHz. Furthermore, it was able to emit radiation at fundamental (1064 nm) and second harmonic. A 150 × optical lens was used to focus the beam on the sample. Stainless steel samples with 1.5 mm thickness were placed on a three-dimensional (3D) motorized translation stage to allow for high-precision (50 nm) positional control. An accurate imaging system using a charge-coupled device (CCD) camera allowed for high-resolution imaging of the ablation zone on the target.

Fig. 1 is a schematic of the picosecond dual-wavelength laser micromachining system used in this study. First, the delay time between the two wavelengths was about 0.5 ns, whereby the visible beam was emitted first, followed by the near-infrared. Furthermore, the index of refraction is higher for the visible beam than the near-infrared [15], so the focal plane of the short-wavelength beam was closer than that of the long-wavelength beam, the distance via experimentation between the two foci was approximately 1.7 mm. The $1/e^2$ focused spot diameters ($2\omega_0$) at each focal plane for the two wavelengths were simultaneously calculated using the following equation:

$$2\omega_0 = \frac{4\lambda f M^2}{\pi d} \tag{1}$$

Table 1
Elemental analysis of SS304 surface using energy dispersive X-ray detector (EDX).

Spectrum (wt%) C	O	Si	Cr	Mn	Fe	Ni
8.28	2.77	0.51	16.72	1.11	62.81	7.80

where ω_0 is the radius of beam waist, λ is the wavelength, f is the focal length of the lens, d is the diameter of the incident beam and M^2 is the beam quality factor [18,19]. Consequently, the focused waist diameter of a Gaussian beam depends on the beam quality and wavelength in the focal plane, which were approximately 64.1 μm and 70.2 μm for the visible beam and near-infrared, respectively. In order to minimize the influence of spots sizes coming from the different wavelengths, likewise, reduce the difference between the two spot diameters, during irradiation the processing surface was set in focal plane of the near-infrared, such that the visible beam produced divergent beam ablation (the divergent distance was about 1.7 mm), resulting in some amplification of the visible beam spot.

Irradiation was carried out under ambient conditions. Various techniques were used to analyze the morphological features of the samples after irradiation, such as scanning electron microscopy (SEM) and laser scanning confocal microscopy (LSCM).

3. Results and discussion

Morphological features of holes and grooves were primarily observed after ablation with the dual-wavelength beam, made up of the visible beam (532 nm) combined with the near-infrared (1064 nm). The results of the induced morphology and geometrical features are presented in the following sections.

3.1. Morphological features of holes ablated by mono-wavelength laser system

A series of experiments was conducted for holes ablation with 10 ps pulse duration, a repetition rate of 1 kHz and the same processing surface. Each beam (the visible beam and the near-infrared) was individually applied at various powers, and then the dual-wavelength beam (combining the visible beam and near-infrared) was applied at different powers combinations.

Fig. 2 shows the SEM images and cross-section profiles of holes on stainless steel surfaces ablated by different wavelengths, demonstrating their dramatically different morphologies. In Fig. 2(A1), which shows a hole ablated by the visible beam with a power of 8 mW, it can be clearly seen that the bottom of the hole was filled with coarse particles and varyingly sized pinholes, most of which had diameters less than 2 μm, at the same time, one larger pinhole with a diameter of about 7 μm appeared in the center of the bottom of the hole. Significant differences were observed for holes ablated by the near-infrared with the same power. As shown in Fig. 2(B1), the bottom of hole consisted of regular ripples and higher-period furrows that were vertical to the ripples. For the visible beam, the side-walls of the holes were mainly composed of symmetrical ravines along the direction of hole depth, otherwise, there was only a small amount of melt ejection, such as debris and droplets, around the hole surface,

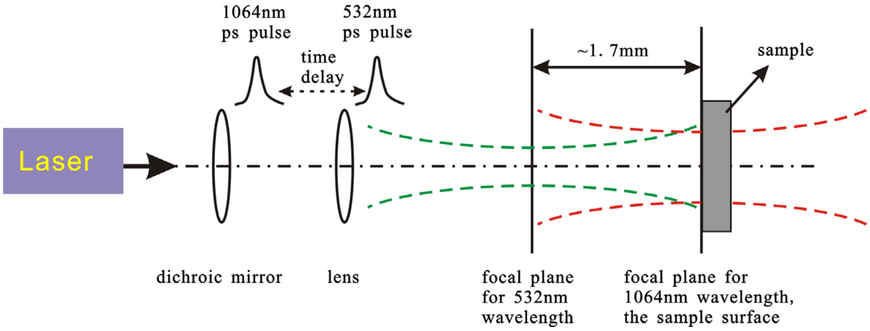

Fig. 1. Schematic of the picosecond dual-wavelength laser micromachining system.